Synthesis and characterization of oxadizole hybrids with nickel nanoparticles

Muqadas Bibi[1], Muhammad Suleman[1], Freeha Hafeez[1*]

Department of Chemistry, Riphah International University Faisalabad

Abstract

Nanoparticles function as the fundamental building blocks utilized within the realm of nanotechnology. Materials containing nanostructures demonstrate exceptional electrical, magnetic, optical, catalytic, and biomedical characteristics when contrasted with conventional bulk materials that are available for purchase. The rise in the use of metal nanoparticles as catalysts in organic reactions has been significant, owing to their efficiency, selectivity, and capacity for multiple uses. 1,3,4-oxadiazoles, which are highly significant due to their diverse applications across various scientific fields such as pharmaceuticals, drug discovery, scintillating material advancement, and the dyestuff sector. The oxadiazole hybrid of diclofenac have been regarded as a potential class of pharmacologically active frame work with a several biological characteristics, such as anti-cancer, anti-alzheimer's, gastro-protective, anti-inflammatory, and anti-cytotoxic agent. The oxadiazole series 184-188 was successfully prepared through the synthesis of diclofenac hydrazide in a reaction yielding 60-85%. Subsequently, their significant anti-cancer properties were evaluated. The identification of the synthetic derivatives' structures was carried out utilizing ^{1}H NMR, melting points, and FT-IR techniques. The evaluation of cytotoxicity for these compounds was conducted by performing in-vitro analysis of hemolysis and thrombolysis. Compound 186 emerged as the most promising among the synthesized derivatives, displaying a RBC lysis percentage of 0.4% and demonstrating minimal toxicity. In contrast, compound 185 exhibited higher thrombolytic potential with a lysis percentage of 67.2%, while the remaining derivatives manifested varying degrees of cytotoxic effects.

Keywords: Anticancer; cytotoxicity**;** diclofenac; nanoparticles; oxadiazole metal complexes; s-stabilized

1. Introduction

Nano catalysis, particularly using transition metal nanoparticles, has advanced due to their superior catalytic activity but is hindered by agglomeration, which reduces their effectiveness [1]. Stabilizing agents prevent this by keeping particles apart through electrostatic, steric, or electrosteric interactions, and ongoing research seeks better, cost-effective solutions [2]. Nanoparticles are utilized as raw materials in the field of nanotechnology [3]. Ni nanoparticles (NiNPs) are highly valued for their unique properties and versatile applications in

catalysis[4], battery manufacture [5], nanotube-printing inks [6], textiles[7], optical devices[8], biomolecule immobilization [9], and dye adsorption [10], offering cost-effective, conductive, and abundant alternatives to other magnetic nanoparticles [11]. Elemental sulfur is rarely used for developing metal nanoparticles, except in synthesizing isolated ligand-capped AuNPs and vulcanized sulfur-AuNPs nanocomposites [12].

As is known, inflammation is a symptom in many common diseases and as an early stage in serious diseases like cancer, cardiovascular diseases, and Alzheimer's [13]. The indications of inflammation involve elevated cellular inflow, blood flow, and edema, increased vasodilation, nitric oxide (NO), reactive oxygen species (ROS), and cellular metabolism [14]. NSAIDs, or non-steroidal anti-inflammatory medicines, are the recommended option for managing different pathological conditions [15]. Diclofenac, an aryl-acetic acid derivative, is a widely used NSAID that inhibits prostaglandin synthesis by blocking COX enzymes [16, 17]. Diclofenac exhibits various biological effects such as antibacterial [18], antitumour [19], and anticancer activities [20, 21]. Diclofenac has been shown to inhibit COX-2 and reduce PGE2 levels, which are often elevated in cancers linked to chronic inflammation [22]. This reduction in PGE2 can inhibit angiogenesis and tumor growth, as seen in BALB/c mice with C-26 adenocarcinoma [23] .

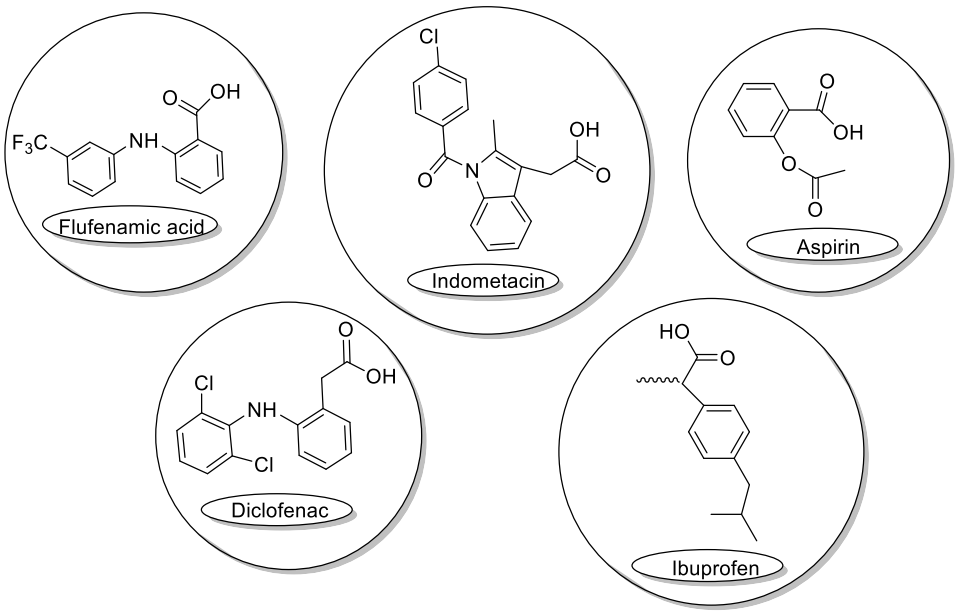

Figure 1: An anti-inflammatory medication with an acidic moiety.

Unfortunately, NSAIDs such as diclofenac and aspirin cause gastrointestinal side effects due to their carboxylic groups interacting with the GI tract, resulting in a pKa of 3.5-5.5 (figure 1) [24, 25]. Various synthetic methods have modified diclofenac's -COOH group to improve its safety and therapeutic window. These modifications, such as using less acidic azoles like 1,3,4-oxadiazole, have enhanced its biological activity [26-28]. In this particular framework, a

sequence of DCF S-stabilised derivatives has been formulated to augment its anti-neoplastic characteristics.

2. Results and Discussion

2.1. Chemistry

Several diclofenac hybrids (5-11) were synthesized in two step process as illustrated in Scheme 1. The process began with the treatment of excess diclofenac sodium with 2N HCl at 0°C in water, which produced the acid derivative of diclofenac 2 in a 100% yield. Next, diclofenac methyl ester 3 was treated with hydrazine hydrate in methanol, yielding the corresponding diclofenac hydrazide 4 95%. The reaction of compound 4 with carbon disulfide (CS_2) and potassium hydroxide inside methanol (MeOH) for 3-4 hours at room temperature produced diclofenac oxadiazole derivatives (5a) with 85% yields. Additionally, oxadiazole 5a was further reacted with metal complexes (7-11) and treated with hydrazine hydrate for 8 hours to produce diclofenac triazole.

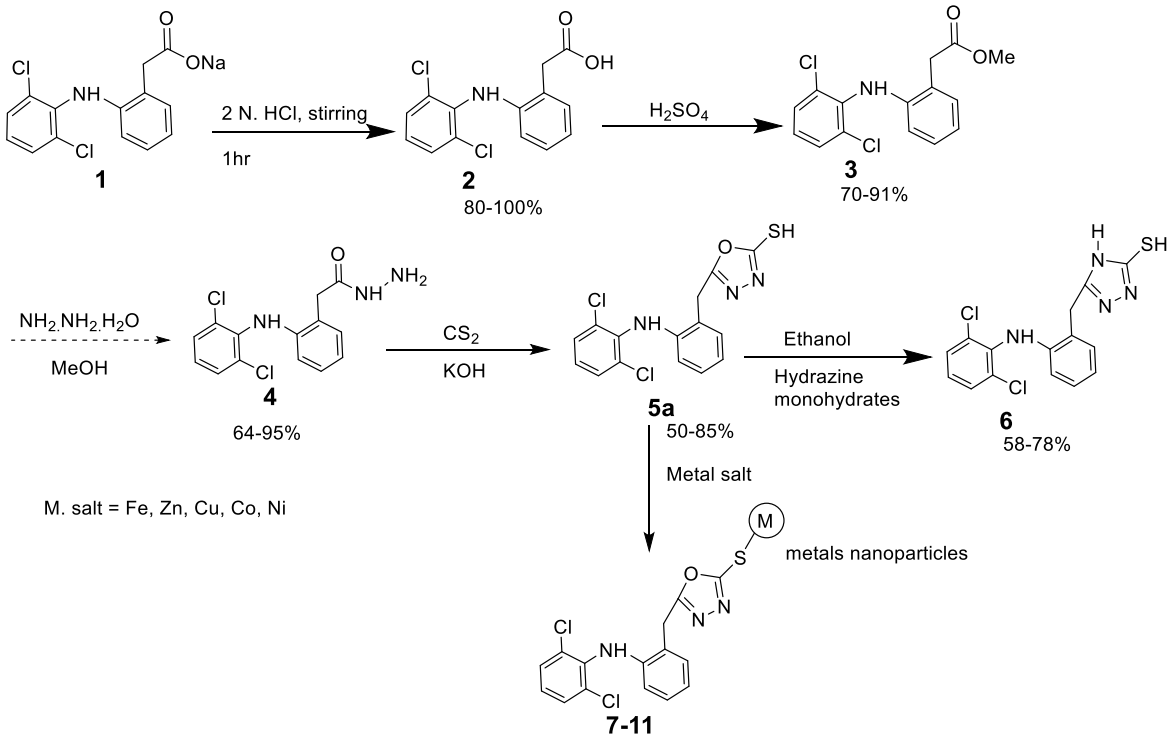

Scheme 1: *A synthetic pathway for the specific compound 7-11 is outlined.*

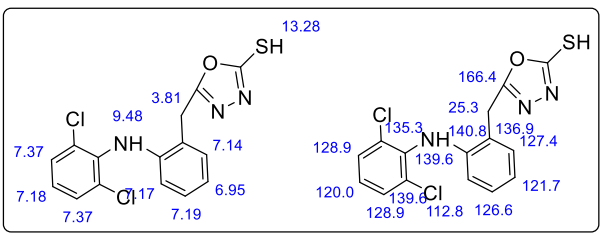

Figure 2: ^{1}H and ^{13}C NMR spectra of compound 5.

The structures of diclofenac based oxadiazole and triazole 1-11 were established using a variety of spectroscopic techniques, and their purity was confirmed by elemental analyses. The FT-IR spectra showed the presence of absorption bands corresponding to the N-H stretching vibrations peak at 3317.97 cm^{-1}, C=C stretching in aromatic compounds appeared at 1583.11 cm^{-1}, symmetric bending of CH_3(methyl) groups peak at 1413.25 cm^{-1}, C-O stretching peak at 1282.22 cm^{-1} and C-O-C stretching peak 1156.95 cm^{-1}.

2.2 Cytotoxic evaluation

2.3 Hemolysis

Compound **186** displayed the least cytotoxicity, whereas compounds **179** and **184** demonstrated the highest level of toxicity. The highest percentage of Red Blood Cell (RBC) lysis was observed in compound **182** at 5.5%, with notable hemolytic effects also seen in compounds **185** (4.7%) and **181** (3.90%).

2.4 Thrombolysis

The thrombolytic activity of synthetic derivatives varied, with compounds **185** and **187** showing higher potential compared to others. Compound **185** demonstrated significant thrombolysis at 67.2%. Derivatives **182** and **186** exhibited lower lysis percentages at 42.1% and 43.05% respectively. Among derivatives **184-188**, compound **186** displayed minimal hemolysis at 0.3%, while compound 185 showed the highest thrombolysis at 67.12%. The modest thrombolytic effects of further derivatives, including **188**(64.2%), **184**(65.1%), and **183** (61.7%) were also shown in these tables. A moderate degree of thrombolytic activity was shown by derivatives **179** (44.1%), **181** (43.28%), and **180** (46.2%).

Table 4.7: *Demonstrates the hemolytic and thrombolytic capabilities of the synthesized compounds 179-183*

Sr. #	Alternatives	Proportion of hemolysis ± SD	The % ± SD of thrombolysis
1	179	2.05 ± 0.111	44.1 ± 0.079
2	180	1.32 ± 0.003	46.2 ± 0.080
3	181	3.90 ± 0.004	43.28 ± 0.007
4	182	5.5 ± 0.040	42.1 ± 0.079
5	183	0.9 ± 0.008	61.7 ± 0.082
Standard	ABTS	96.8	87

Sr. #	Alternatives	Proportion of hemolysis ± SD	The % ± SD of thrombolysis
1	184	5.11 ± 0.03	65.1 ± 0.071
2	185	4.7 ± 0.044	67.2 ± 0.091
3	186	0.3 ± 0.003	43.05 ± 0.009
4	187	1.7 ± 0.018	66.5 ± 0.079
5	188	0.9 ± 0.013	64.2 ± 0.80
Standard	ABTS	95.8	84

The Mean ± Standard Deviation was determined in triplicate at a concentration of micrograms per milliliter. Dimethyl sulfoxide (DMSO) and 2,2'-azino-bis(3-ethylbenzothiazoline-6-sulphonic acid) (ABTS) were employed as the negative and positive controls, respectively.

The tables provided additional evidence of the subtle thrombolytic impacts of various other derivatives, including **184** (65.1%), **188** (64.2%), and **183** (61.7%). Derivatives **179** (44.1%), **181** (43.28%), and **180** (46.2%) exhibited a moderate degree of thrombolytic efficacy.

Table 4.8: *The synthetic compounds 184-188 demonstrate both hemolytic and thrombolytic activities*

Mean ± standard deviation was calculated in triplicate using a concentration of micrograms per milliliter. Dimethyl sulfoxide (DMSO) and 2,2'-azino-bis(3-ethylbenzothiazoline-6-sulfonic acid) (ABTS) were employed as the negative and positive controls, respectively.

3. Material and methods

3.1. General

Solvents and chemicals procured from E. Merck Germany were distilled at least once before use. ^{1}H-NMR spectra were obtained using a 400 MHz AV-400 spectrometer with $CDCl_3$ as the solvent, quantified at 7.26 ppm. MestReC software was used for spectral analysis, with δ-values recorded in ppm. ^{13}C-NMR spectra were also captured on the AV-400 spectrometer at 100 MHz, with $CDCl_3$ as the solvent, quantified at 77.0 ppm, and analyzed using MestReC software. Characterization included FT-IR analysis using the Perkin Elmer Spectrum GX FT-IR system. Thin layer chromatography was performed on pre-coated polygram® SIL-G/UV 254 plates from Fluke, with spots viewed under UV light.

3.2. General procedure for the synthesis of diclofenac derivatives 5-11

2-(2-(amino)phenyl)(2,6-dichlorophenyl)acetic acid (**2**)

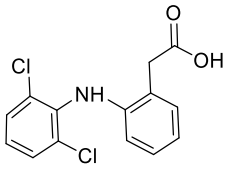

Yield 100%, m.p. 151-154°C. m/z: 294.01. ^{13}C NMR: CH_2 (28.1), Ar-C (118.6), (120.0), (125.2), (127.0), (127.1), (128.4), (128.9), (135.3), (139.6), C=O (176.2). ^{1}H-NMR: (s, 2H, CH_2)3.69, (dd, 1H, Ar-H)6.76, (d, 1H, Ar-H)7.15, (d, 1H, Ar-H)7.18, (dd, 1H, Ar-H) 7.18, (dd, 1H, Ar-H)7.299, (d, 2H, Ar-H)7.37, (s, 1H, amide)9.48, (s, 1H, OH)12.39.

Methyl 2-(2-(amino)phenyl)(2,6-dichlorophenyl)acetate (**3**)

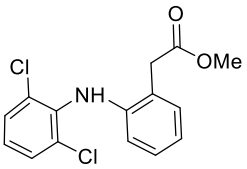

Yield 91%, m.p. 97-100°C. m/z: 295.02. ^{13}C NMR: CH_2 (35.6), C-O-C (51.9), Ar-C (118.6), (120.0), (125.2), (127.0), (127.1), (128.4), (128.9), (135.3), (139.6), C=O (171.2). ^{1}H-NMR: (s, 3H, CH_3)3.66, (s, 2H, CH_2)3.71, (dd, 1H, Ar-H)6.76, (d, 1H, Ar-H)7.15, (dd, 1H, Ar-H) 7.18, (dd, 1H, Ar-H)7.299, (d, 2H, Ar-H)7.37, (s, 1H, amide) 9.48

2-(2-(amino)phenyl((2,6-dichlorophenyl))aceto-hydrazide (**4**)

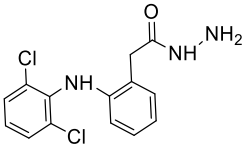

Yield 95%, m.p. 133-134°C. m/z: 309.04. ^{13}C-NMR: CH_2 (37.4), Ar-C (118.7), (120.0), (126.1), (126.9), (127.2), (128.5), (128.9), (135.3), (139.6), C=O 168.1. ^{1}H-NMR: (s, 2H, CH_2)3.70, (d, 2H, NH_2)4.22, (dd, 1H, aryl)6.76, (d, 1H, aryl)7.15, (d, 1H, aryl)7.17, (dd, 1H aryl)7.18, (dd, 1H, aryl)7.29, (d, 2H, aryl)7.37, (t, 1H, NH)9.08, (s, 1H, NH)9.48.

5-(2-((amino)benzyl(2,6-dichlorophenyl))-1,3,4-oxadiazole-2-thiol (**5**)

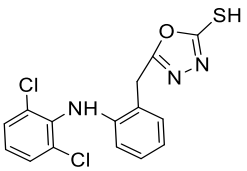

Yield 85%, m.p. 159-162°C. m/z: 351.00. IR: ν (cm^{-1}): CH_3 (1413.25 cm^{-1}), N-H (3317.97 cm^{-1}), C=C (1583.11 cm^{-1}), C-O (1282.22 cm^{-1}), and C-O-C (1156.95 cm^{-1}). ^{13}C-NMR: 500MHz,

$CDCl_3$, CH_2 (25.3), Ar-C (112.8), (120.0), (121.7), (126.6), (127.4), (128.9), (135.3), (136.9), (139.6), (140.8), C=N (166.4) C=N-S 175. ^{1}H-NMR: (s, 2H, CH_2)3.81, (dd, 1H, aryl)6.95, (d, 1H, aryl)7.14, (d, 1H, aryl)7.17, (dd, 1H, aryl)7.18, (dd, 1H, aryl)7.19, (d, 2H, aryl)7.37, (s, 1H, NH)9.48, (s, 1H, SH)13.28.

5-(2-((amino)benzyl(2,6-dichlorophenyl)-4H-1,2,4-triazole-3-thiol) (**6**)

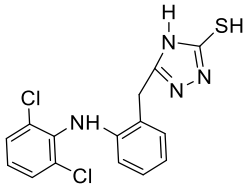

Yield 78%, m.p. 253-256°C. m/z: 350.02. IR: ν (cm^{-1}): N-H (3331.75 cm^{-1}), C=O (1680.80 cm^{-1}), C-H (1440.00cm^{-1}), C-O (1288.03 cm^{-1}) and C-O-C (1156.89 cm^{-1}). ^{13}C NMR: CH_2 (28.7) Ar-C (112.8), (120.0), (121.7), (126.6), (127.4), (128.9), (135.3), (136.9), (139.6), (140.8), C=N (159.3), N=C-S (158.6). ^{1}H-NMR: (s, 2H, CH_2)3.81, (dd, 1H, aryl)6.95, (d, 1H, aryl)7.14, (d, 1H, aryl)7.17, (dd, 1H, aryl)7.18, (dd, 1H, aryl)7.19, (d, 2H, aryl)7.37, (s, 1H, NH)9.48, (s, 1H, SH)13.28.

nickel 5-(2-((amino)benzyl(2,6-dichlorophenyl))-1,3,4-oxadiazole-2-thiolate (**7**)

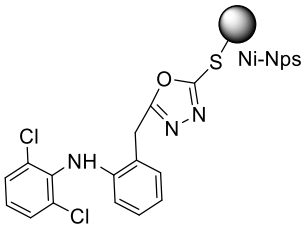

Yield 92%, ^{13}C-NMR: 500MHz, $CDCl_3$, CH_2 (25.3), Ar-C (112.8), (120.0), (121.7), (126.6), (127.4), (128.9), (135.3), (136.9), (139.6), (140.8), C=N (166.4) C=N-S 175. ^{1}H-NMR: (s, 2H, CH_2)3.81, (dd, 1H, aryl)6.95, (d, 1H, aryl)7.14, (d, 1H, aryl)7.17, (dd, 1H, aryl)7.18, (dd, 1H, aryl)7.19, (d, 2H, aryl)7.37, (s, 1H, NH)9.48, (s, 1H, SH)13.28.

Calcium (I) 5-(2-((amino)benzyl(2,6-dichlorophenyl))-1,3,4-oxadiazole-2-thiolate (**8**)

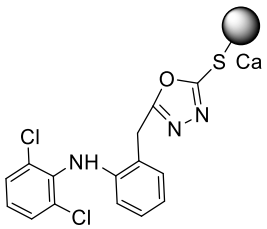

Yield 86%, ^{13}C-NMR: 500MHz, $CDCl_3$, CH_2 (25.3), Ar-C (112.8), (120.0), (121.7), (126.6), (127.4), (128.9), (135.3), (136.9), (139.6), (140.8), C=N (166.4) C=N-S 175. ^{1}H-NMR: ^{1}H-NMR: (s, 2H, CH_2)3.81, (dd, 1H, aryl)6.95, (d, 1H, aryl)7.14, (d, 1H, aryl)7.17, (dd, 1H, aryl)7.18, (dd, 1H, aryl)7.19, (d, 2H, aryl)7.37, (s, 1H, NH)9.48, (s, 1H, SH)13.28.

1,3,4-oxadiazol 2((5(2((2,6dichlorophenyl)amino)benzyl)yl)thio) copper (**9**)

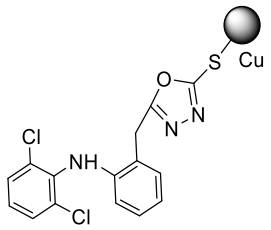

Yield 89%, ^{13}C-NMR: 500MHz, $CDCl_3$, CH_2 (25.3), Ar-C (112.8), (120.0), (121.7), (126.6), (127.4), (128.9), (135.3), (136.9), (139.6), (140.8), C=N (166.4) C=N-S 175. ^{1}H-NMR: (s, 2H, CH_2)3.81, (dd, 1H, aryl)6.95, (d, 1H, aryl)7.14, (d, 1H, aryl)7.17, (dd, 1H, aryl)7.18, (dd, 1H, aryl)7.19, (d, 2H, aryl)7.37, (s, 1H, NH)9.48, (s, 1H, SH)13.28.

1,3,4-oxadiazol-2((5(2((2,6dichlorophenyl)amino)benzyl)yl)thio) iron (**10**)

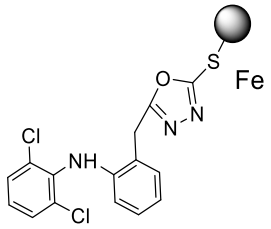

Yield 80%, ^{13}C-NMR: 500MHz, $CDCl_3$, CH_2 (25.3), Ar-C (112.8), (120.0), (121.7), (126.6), (127.4), (128.9), (135.3), (136.9), (139.6), (140.8), C=N (166.4) C=N-S 175. ^{1}H-NMR: (s, 2H, CH_2)3.81, (dd, 1H, aryl)6.95, (d, 1H, aryl)7.14, (d, 1H, aryl)7.17, (dd, 1H, aryl)7.18, (dd, 1H, aryl)7.19, (d, 2H, aryl)7.37, (s, 1H, NH)9.48, (s, 1H, SH)13.28.

1,3,4-oxadiazol-2-((5-(2-((2,6-dichlorophenyl)amino)benzyl)yl)thio) zinc (**11**)

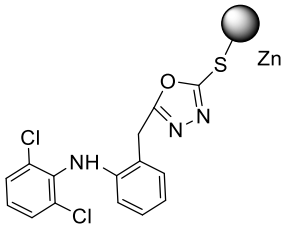

Yield 84%, ^{13}C-NMR: 500MHz, $CDCl_3$, CH_2 (25.3), Ar-C (112.8), (120.0), (121.7), (126.6), (127.4), (128.9), (135.3), (136.9), (139.6), (140.8), C=N (166.4) C=N-S 175. ^{1}H-NMR: (s, 2H, CH_2)3.81, (dd, 1H, aryl)6.95, (d, 1H, aryl)7.14, (d, 1H, aryl)7.17, (dd, 1H, aryl)7.18, (dd, 1H, aryl)7.19, (d, 2H, aryl)7.37, (s, 1H, NH)9.48, (s, 1H, SH)13.28.

Cytotoxic assay

The evaluation of cytotoxicity for the generated compounds was carried out via in vitro examination involving hemolysis and thrombolysis investigations.

3.6.1 Hemolysis

In a vessel containing EDTA, a 5ml fresh blood specimen was acquired from a healthy contributor. Subsequent to the blood procurement into microcentrifuge receptacles, the centrifugation process of red blood cells (RBCs) took place for a duration of 5 minutes at 1000 rpm. The supernatant was subsequently decanted, followed by a series of three washes with PBS (phosphate buffer saline) on the RBC sediment. Following the rinsing process, retrieval of the RBC sediment was executed, and 20 µL of sample solution in DMSO was introduced. The receptacles were subjected to a 60-minute incubation period at a temperature of 37°C. Subsequent to the removal of the receptacles from the incubation apparatus, a re-centrifugation was conducted at 13000 rpm for 5 minutes. The harvested supernatant was diluted with chilled phosphate buffer saline and the optical density was determined at 517 nm. In this particular experimental arrangement, DMSO functioned as the negative standard, whereas ABTS was designated as the positive standard [29]. This technique was employed to ascertain the extent of RBC disintegration in the experimental protocols, all of which were replicated in triplicate.

$$\text{RBC's Lysis (\%)} = \frac{\boldsymbol{absorbance\ of\ sample - absorbance\ of\ negative\ control}}{\boldsymbol{absorbance\ of\ positive\ control}} \times \mathbf{100}$$

3.6.2 Thrombolysis

The methodology employed in this study involved the use of the literature approach to conduct thrombolytic assays [30]. A blood sample of 3 ml was obtained from a healthy human donor and 500 µL was then transferred to pre-cleaned and pre-weighed eppendorf tubes. These tubes were subsequently filled with blood and underwent an incubation period at 37°C for one hour to monitor clot formation. Following the removal of serum, the tube containing the clot was weighed. The clot was then treated with 40 µL of the sample solution in DMSO during an additional 3-hour incubation at 37°C to assess lysis outcomes. It should be emphasized that DMSO acted as the negative control, whereas ABTS functioned as the positive control in this specific experimental setup. The experiments were conducted in triplicate, utilizing a designated formula for the calculation of lysis percentage.

$$\text{Percentage of clot lysis} = \frac{\boldsymbol{initial\ clot\ weight - final\ clot\ weight}}{\boldsymbol{initial\ clot\ weight}} \times \mathbf{100}$$

Statistical Analysis

Trials were conducted in triplicate, and outcomes were depicted as the mean ± standard deviation (SD). The statistical analysis was carried out utilizing Microsoft Excel 2010. The assessments were subjected to scrutiny through a one-way analysis of variance (ANOVA).

Levels of significance were determined among the entities at $p < 0.05$, with the information being displayed as mean ± standard error (SE).

Conclusions

In this study, nine analogs of diclofenac were synthesized using recent synthetic approach and anticancer activities of diclofenac 5 and its derivatives were performed. Five derivatives were found to be active. Diclofenac derivatives 5, 6, 7, 8, 9, 10 and 11 shown a more effective cytotoxic impact than pristine DCF against Hep-G2, HT29, and B16-F10 cancer cells. Overall, 4 exhibits promising outcomes and has potential for creating enhanced medications for cancer treatment. The target molecules (5-11) were evaluated for their anticancer activity via hemolysis and thrombolysis. Among all the synthesized molecules, compound 8 emerged as the most promising among the synthesized derivatives, displaying a RBC lysis percentage of 0.4% and demonstrating minimal toxicity. In contrast, compound 7 exhibited higher thrombolytic potential with a lysis percentage of 67.2%, while the remaining derivatives manifested varying degrees of cytotoxic effects represents effective lead derivative for future studies.

ACKNOWLEDGEMENT

The authors express their gratitude to the Higher Education Commission (HEC) of Pakistan and Riphah International university Faisalabad, Pakistan for the provision of facilities essential for conducting this research.